

## FeSi/IrMn Exchange-Coupled Multilayer Film with Plural FMR Absorptions

Makoto Sonehara, Toshiro Sato, Kiyohito Yamasawa, Yoshimasa Miura  
and Masahiro Yamaguchi \*

Faculty of Engineering, Shinshu University, 4-17-1 Wakasato, Nagano 380-8553, Japan  
Fax: 81-26-223-7754, e-mail: max.@yslab.shinshu-u.ac.jp

\* Graduate School of Engineering, Tohoku University, 05 Aoba, Sendai 980-8579, Japan  
Fax: 81-022-263-9410, e-mail: yamaguti@ecei.tohoku.ac.jp

FeSi/IrMn exchange-coupled multilayer films for wideband noise filter were fabricated and evaluated. The FeSi film had a high saturation magnetization of 19 kG and a low magnetostriction of the order of  $10^{-6}$ . Since the exchange bias magnetic field is introduced to the ferromagnetic FeSi layers by FeSi/IrMn exchange coupling, higher ferromagnetic resonance (FMR) frequency was obtained. In addition, the FeSi/IrMn exchange-coupled multilayer film with different thickness in each FeSi layer exhibited the plural FMRs. The plural FMRs mean the wideband energy absorption, and enable to apply to thin film material with wideband noise absorption for wideband noise filter used in GHz frequency range.

**Key words:** Exchange coupling, FeSi/IrMn, plural FMR absorptions, noise filter

## 1. INTRODUCTION

Electromagnetic interference (EMI) has become extremely important problem in the various electronic instruments such as personal computer, USB high-speed digital signal interface, and others. Recently, Yamaguchi et al. [1] reported a GHz band thin-film noise suppressor with a CoZrNb ferromagnetic thin film array. The device based on the ferromagnetic resonance (FMR) absorption in the GHz frequency range.

In this study, an FeSi/IrMn exchange-coupled multilayer film has been proposed as the ferromagnetic resonance absorption material for GHz band noise filter. Fundamental idea, fabrication and characterization of the films are described in the following sections.

## 2. FUNDAMENTAL IDEA

### 2.1 Ferromagnetic resonance absorption

When a frequency of an external ac magnetic field for ferromagnetic material corresponds to spin precession frequency, the ferromagnetic resonance (FMR) occurs. The FMR frequency  $f_r$  of the ferromagnetic film with uniaxial magnetic anisotropy is written as follows [2],

$$f_r = \frac{\gamma}{2\pi} \{H_k (H_k + M_s)\}^{1/2} \quad (1),$$

where  $\gamma$  is the gyromagnetic constant,  $H_k$  is the uniaxial anisotropy magnetic field, and  $M_s$  is the saturation magnetization. At the FMR point, the permeability becomes unity. The imaginary part of permeability  $\mu_r''$  means the energy absorption, and the maximum value  $\mu_r''(\text{max.})$  at the FMR point can be expressed as follows [3],

$$\mu_r''(\text{max.}) = \chi_s \frac{f_r}{2\lambda}, \quad \chi_s = \frac{M_s}{H_k} \quad (2)$$

where  $\lambda$  is the relaxation frequency, and  $\chi_s$  is the static magnetic susceptibility.  $\lambda$  is in proportion to the damping factor  $\alpha$  for spin rotation, where  $\alpha$  is ordinarily 0.01 to 0.02 for the various ferromagnetic materials.

### 2.2 Eddy current effect in metallic film

In the metallic ferromagnetic film, although the energy absorption due to the eddy current is also generated in the high frequency range, the maximum absorption  $\mu_r''(\text{max.})$  at the FMR point becomes smaller than the intrinsic FMR absorption  $\mu_r''(\text{max.})$ .  $\mu_r''(\text{max.})$  is shown in the next equation [4].

$$\mu_r''(\text{max.}) = \frac{\mu_r''(\text{max.})}{Z} \cdot \frac{\sinh Z - \sin Z}{\cosh Z + \cos Z} \quad (3),$$

$$Z = \frac{t_m}{S_{r(\text{min.})}}, \quad S_{r(\text{min.})} = \left\{ \frac{\rho}{\omega \mu_r''(\text{max.})} \right\}^{1/2}$$

where  $t_m$  is the film thickness,  $\rho$  is the resistivity of the film material.  $S_{r(\text{min.})}$  means the minimum skin depth at the FMR point, which is due to the maximum  $\mu_r''$  ( $\mu_r''(\text{max.})$ ) at the FMR point. This phenomenon is called "Skin effect anomaly due to the FMR" [5]. If the minimum skin depth  $S_{r(\text{min.})}$  is much smaller than the film thickness  $t_m$  ( $Z \gg 1$ ),  $\mu_r''(\text{max.})$  becomes much smaller than  $\mu_r''(\text{max.})$ .

Fig. 1 shows the examples of the frequency spectra of the energy absorptions with and without skin effect. The peak energy absorption in the conductive material becomes smaller than the intrinsic maximum FMR absorption. Although thinner metallic film with small skin effect exhibits near characteristic of the intrinsic FMR absorption, the frequency bandwidth of the intrinsic absorption is narrow. The ferromagnetic film for wideband noise filter is desired to have wideband energy absorption and large peak value.

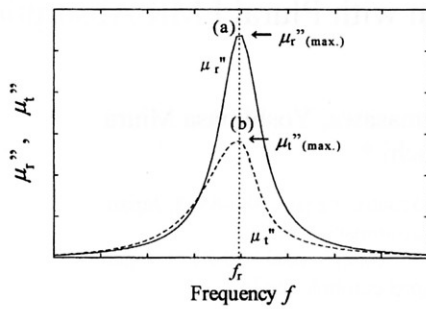


Fig. 1 Schematic illustration of energy absorption versus frequency, (a) is the intrinsic FMR absorption, (b) is an effect of skin effect in conductive material.

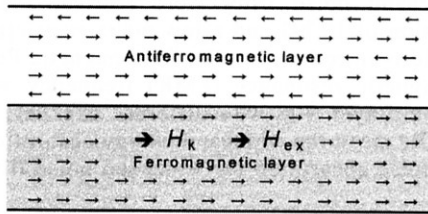


Fig. 2 Ferro/antiferro exchange-coupled bilayer film.

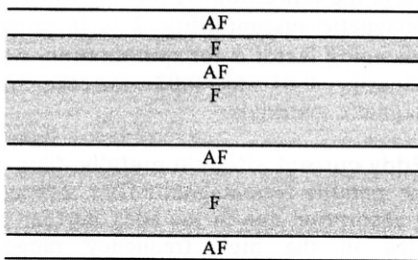


Fig. 3 Ferro/antiferro exchange-coupled multilayer film with different thickness ferromagnetic layer.

### 2.3 Ferro/antiferro exchange-coupled film

Recently, the ferro/antiferro exchange-coupled films have been developed [6, 7], which will be expected for soft underlayers for perpendicular magnetic recording media. The authors have also studied a ferro/antiferro exchange-coupled film for high frequency devices [8]. When the exchange bias magnetic field  $H_{ex}$  for the ferromagnetic layer is aligned in the easy magnetization direction, the FMR frequency increases according to the following equation,

$$f_r = \frac{\gamma}{2\pi} \{ (H_k + H_{ex})(H_k + H_{ex} + M_s) \}^{1/2} \quad (4),$$

Comparing (4) with (1), the FMR frequency of the exchange-coupled ferromagnetic film becomes higher than the intrinsic one. Therefore, the film will be expected as the high frequency magnetic materials with higher FMR frequency.

### 2.4 Ferro/antiferro exchange-coupled film with plural FMR absorptions

The exchange bias magnetic field  $H_{ex}$  in the ferro/antiferro bilayer film (shown in Fig. 2) is inversely proportional to the ferromagnetic layer thickness  $t_F$  [9],

$$H_{ex} = J_{ex} / M_s t_F \quad (5),$$

where  $J_{ex}$  is the exchange energy at the ferro/antiferro interface. The FMR frequency  $f_r$  can be controlled by ferromagnetic layer thickness  $t_F$ . In the ferro/antiferro exchange-coupled multilayer film with different thickness of each ferromagnetic layer, as shown in Fig. 3, the different exchange bias magnetic field will occur in each ferromagnetic layer. In this case, since the intermediate ferromagnetic layers are coupled to both the upper and lower antiferromagnetic layers, the exchange biasing  $H_{ex(i)}$  for each intermediate ferromagnetic layer can be written as follows,

$$H_{ex} = 2J_{ex} / M_s t_F \quad (6),$$

Therefore, the multilayer film with various exchange biasing for each ferromagnetic layer exhibits the plural FMRs, that is, plural FMR absorptions. By using the plural FMRs with plural maximum energy absorptions, the wideband energy absorption will be expected for wideband noise suppression devices.

## 3. EXPERIMENTALS

### 3.1 Fabrication of films

FeSi/IrMn exchange-coupled multilayer film for wideband energy absorption material was fabricated and characterized. The FeSi film had a high saturation magnetization of 19 kG, a low magnetostriction of the order of  $10^{-6}$ , and an electrical resistivity of  $75 \mu\Omega\text{cm}$  [10]. An IrMn with the electrical resistivity of  $200 \mu\Omega\text{cm}$  [9] was used as the antiferromagnetic film.

FeSi and IrMn films were fabricated by using RF magnetron sputtering machine (ANELVA; SPF-313). The (100)Si with thin  $\text{SiO}_2$  surface was used as the substrate. The films were deposited under applying dc magnetic field of 140 Oe. Table 1 shows the sputtering conditions for FeSi and IrMn films.

Though not shown in detail here, in the FeSi/IrMn multilayer films, the (110) preferential orientation for FeSi layer and the (111) preferential orientation for IrMn layer were observed by the X-ray diffractometry measurement. Since the magnetic moment of the IrMn film lags in the (111) plane, the exchange coupling at the FeSi/IrMn interface can be expected. In the fabricated films, however, the exchange coupling was obtained only when the FeSi film was used as the most bottom layer on  $\text{SiO}_2/\text{Si}$  substrate. This reason is currently unknown.

The resistivity of IrMn was about 3 times higher than that of FeSi. In addition, each FeSi

Table 1 Sputtering conditions of FeSi and IrMn films.

	FeSi	IrMn
	3" Target	6 wt.%Si-Fe
Base pressure	< $9 \times 10^{-5}$ Pa	
Ar pressure	0.7 Pa	0.7 Pa
RF power	200 W	300 W
Deposition rate	0.1 nm/s	0.8 nm/s
Remarks	Substrate rotation -----	

Substrate ; (100)Si with surface  $\text{SiO}_2$

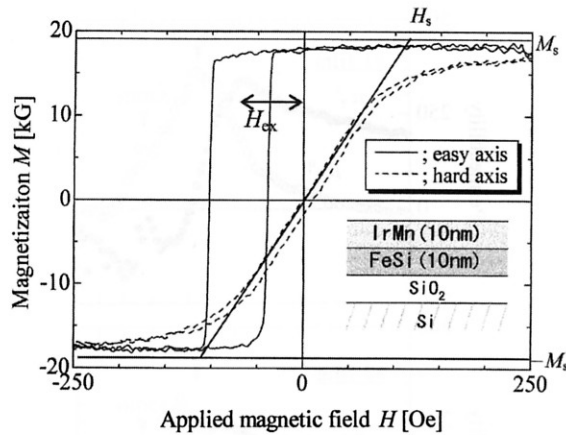


Fig. 4 Static magnetization curves measured in IrMn(10nm)/FeSi(10nm)/SiO<sub>2</sub>/Si.

layer thickness in the fabricated FeSi/IrMn multilayer film was thin enough (4 – 25 nm). Hence, it was considered that the skin effect in each thin FeSi layer was negligibly small.

3.2 Magnetic properties

Static magnetization curves in the fabricated films were evaluated by using a vibrating sample magnetometer (Riken Electronics Co., BHV-55). High frequency complex permeability was measured by using a thin film permeance meter developed by M. Yamaguchi et al. [11].

4. RESULTS AND DISCUSSION

4.1 FeSi/IrMn bilayer film

Fig. 4 shows the static magnetization curves measured in the IrMn(10nm)/FeSi(10nm) bilayer film. From the result, the exchange bias magnetic field  $H_{ex}$  in easy axis was estimated to be about 70 Oe, and the saturation magnetic field  $H_s$  in hard axis was estimated to be about 110Oe.

Fig. 5 shows the relation between exchange bias magnetic field  $H_{ex}$ , saturation magnetic field  $H_s$  and FeSi film thickness  $t_F$ , where thickness  $t_{AF}$  of antiferromagnetic IrMn film was kept to 10nm. From result of Fig. 5,  $H_{ex}$  was nearly inversely proportional to  $t_{AF}$ , and exchange energy  $J_{ex}$  of FeSi/IrMn interface was estimated to be about 0.1 erg/cm<sup>2</sup>, which was comparable with that of FeTaN/IrMn by H. S. Jung et al. [6]. The difference between  $H_s$  and  $H_{ex}$  means the intrinsic uniaxial anisotropy magnetic field  $H_k$  of FeSi layer. From result of  $H_s$  and  $H_{ex}$  in Fig. 5, the intrinsic  $H_k$  was estimated to be about 40 Oe.

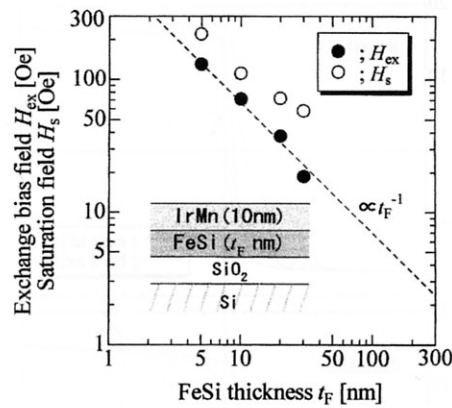


Fig. 5 Relation between FeSi film thickness  $t_F$  and exchange bias field  $H_{ex}$ , saturation field  $H_s$  in IrMn(10nm)/FeSi( $t_F$ )/SiO<sub>2</sub>/Si.

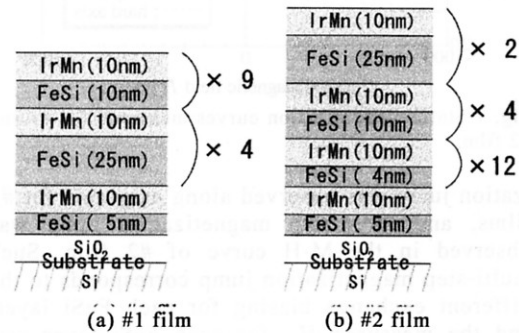


Fig. 6 Two kinds of multilayer films with plural FMRs, #1 is expected to have two FMRs, #2 is expected to have three FMRs.

4.2 FeSi/IrMn multilayer film

In order to investigate the characteristics of the FeSi/IrMn multilayer film with plural FMRs, two kinds of films were fabricated. Fig. 6 shows the film structures fabricated here. Two films consisted of some intermediate FeSi layers and the most bottom FeSi layer. The reason for the most bottom FeSi layer is described in 3.1.

Table 2 shows the each layer thickness in two multilayer films fabricated. #1 film had two kinds of intermediate FeSi thickness  $t_{F(i)}$ , and #2 film had three kinds of FeSi thickness  $t_{F(i)}$ . In Table 2, the values in parentheses show the predicted  $H_{ex}$ ,  $H_s$  and  $f_i$  in each FeSi layer.

Fig. 7 shows the static magnetization curves measured for #1 and #2 films. Two-step magnet-

Table 2 FeSi and IrMn layer thickness of two kind of multilayer films fabricated.

	#1 film with two FMR points	#2 film with three FMR points
Intermediate FeSi layer thickness $t_{F(i)}$	25 nm × 4 layer ( 56 Oe, 96 Oe, 3.8 GHz ) 10 nm × 9 layer (140 Oe, 180 Oe, 5.2 GHz )	25 nm × 2 layer ( 56 Oe, 96Oe, 3.8 GHz ) 10 nm × 4 layer (140 Oe, 180Oe, 5.2 GHz ) 4 nm × 12 layer (350 Oe, 390 Oe, 7.7 GHz )
Bottom FeSi layer thickness $t_{F(b)}$	5 nm (140 Oe, 180 Oe, 5.2 GHz )*	5 nm (140 Oe, 180 Oe, 5.2 GHz )*
IrMn layer thickness $t_{AF}$	10nm	
Total thickness $t$	335 nm	333 nm

Substrate ; (100)Si with surface SiO<sub>2</sub>. Values in parentheses; Predicted  $H_{ex}$ ,  $H_s$  and  $f_i$  in each FeSi, that is, ( $H_{ex}$ ,  $H_s$ ,  $f_i$  ).

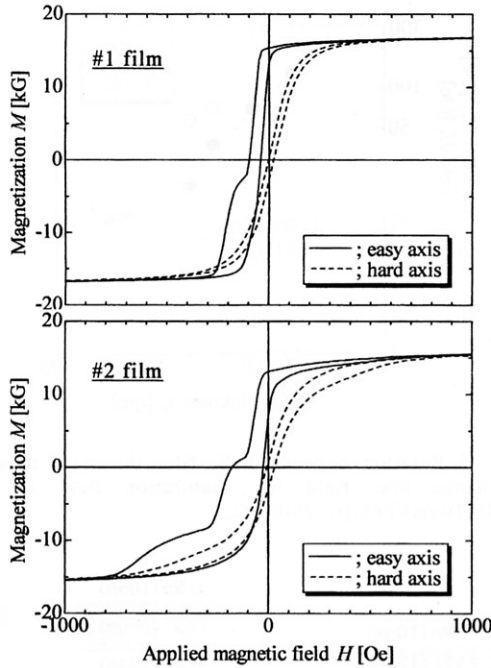


Fig. 7 Static magnetization curves measured for #1 and #2 film.

ization jump was observed along easy axis for #1 films, and three-step magnetization jump was observed in the M-H curve of #2 film. Such multi-step magnetization jump corresponds to the different exchange biasing for each FeSi layer, and the measured  $H_{ex}$  for each FeSi layer was nearly same as the predicted ones shown in Table 2.

Fig. 8 shows the frequency dependence of the complex permeability ( $\mu' - j\mu''$ ) measured for #1 and #2 films. The peak absorption  $\mu''_{(max.)}$  of #1 film was observed at around 3.8 GHz, and this frequency was equal to the calculated one for 25 nm FeSi  $\times$  4 layer. Second peak absorption due to 10 nm thick intermediate FeSi and bottom 5 nm thick FeSi, which was predicted at 5.2 GHz, was not clearly observed. The authors consider that the observed  $\mu''$  profile consists of two FMR absorptions, one was the first FMR at 3.8 GHz, the other was the second FMR at 5.2 GHz. #2 film exhibited a broad  $\mu''$  profile, which consisted of three FMR absorptions including third FMR at 7.7 GHz.

## 5. Conclusion

FeSi/IrMn exchange-coupled multilayer films for wideband noise filter were fabricated and evaluated. The multilayer films with different thickness intermediate FeSi layer exhibited the plural exchange biasing for each FeSi layer. The fabricated two types of the multilayer films exhibited the wideband energy absorptions in the GHz frequency band, which composed of the plural FMR absorptions. Therefore, FeSi/IrMn multilayer film with plural FMR absorptions will be suitable for wideband noise filter used in GHz frequency band.

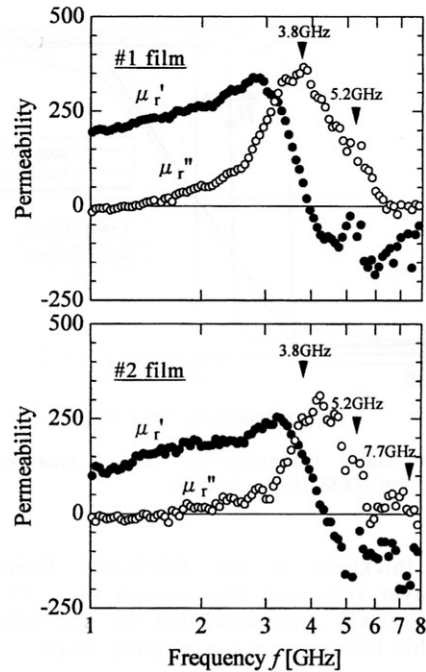


Fig. 8 Frequency dependence of complex permeability measured for #1 and #2 films.

## References

- [1] M. Yamaguchi, K.-H. Kim, T. Kuribara, and K.-I. Arai, "Thin-Film RF Noise Suppressor Integrated in a Transmission Line", *IEEE Transactions Magnetics*, Vol. 38, No.5, (Sept. 2002), pp. 3183-3185.
- [2] K. Ohta, "Fundamental of Magnetics II", *Kyoritsu Syuppan Co.*, (1976), pp. 350-352.
- [3] S. Iida, Y. Sakurai, S. Iwasaki, T. Nagashima, Y. Iwama, S. Watanabe, H. Kobayashi, "Magnetic Thin Film Technology", *Maruzen Co.*, (1972), pp. 150-158.
- [4] T. Sato, H. Tomita, A. Sawabe, T. Inoue, T. Mizoguchi, M. Sahashi, "A magnetic thin film inductor and its application to a MHz switching dc-dc converter", *IEEE Transactions on Magnetics*, Vol. 30, No. 2, (March 1994), pp. 217-223.
- [5] T. Sato, S. Ikeda, H. Nakayama, K. Takizawa, K. Yamasawa, "Relation between power dissipation and signal transmission characteristic in CoZrNb/ polyimide hybrid microstrip line", *Transactions of the Magnetics Society of Japan*, Vol. 2, No. 5, (2002), pp. 377-383.
- [6] H. S. Jung, W. D. Doyle, "FeTaN/IrMn exchange-coupled multilayer films as soft underlayers for perpendicular media", *IEEE Transactions on Magnetics*, Vol. 37, No. 4, (2001), pp.2294-2297.
- [7] H. S. Jung, W. D. Doyle, "CoFe/IrMn exchange-coupled soft underlayers for perpendicular media", *IEEE Transactions on Magnetics*, Vol. 38, No. 5, (2002), pp.2015-2017.
- [8] M. Sonohara, T. Sato, K. Yamasawa, "Preparation and evaluation of FeSi/IrMn exchange-coupled multilayer thin films for micromagnetic devices in GHz band", *Technical Report of IEE of Japan*, MAG-03-17, (2003), pp. 19-24.
- [9] M. Jimbo, "Present status of antiferromagnetic materials in spin valves", *Journal of Magnetics Society of Japan*, Vol. 22, No. 1, (1988), pp.12-18.
- [10] K.-I. Arai, et al., "Magnetics -Fundamentals and Applications-", *CORONA PUBLISHING CO.*, (1999), p.62.
- [11] M. Yamaguchi, Y. Miyazawa, K. Kaminishi, K.-I. Arai, "A new 1MHz - 9GHz thin-film permeameter", *IEEE International Magnetics Conference*, (2003), EA-03.